ACS Sustainable Chemistry & Engineering

Research Article

pubs.acs.org/journal/ascecg

High Efficiency in Energy Generation from Salinity Gradients with Reverse Electrodialysis

David A. Vermaas,[†,‡] Joost Veerman,[§] Ngai Yin Yip,[∥] Menachem Elimelech,[∥] Michel Saakes,[†] and Kitty Nijmeijer*[,‡]

[†]Wetsus, Centre of Excellence for Sustainable Water Technology, P.O. Box 1113, 8900 CC, Leeuwarden, The Netherlands

[‡]Membrane Science & Technology, University of Twente, MESA+ Institute for Nanotechnology, P.O. Box 217, 7500 AE, Enschede, The Netherlands

[§]REDstack B.V., Pieter Zeemanstraat 6, 8606 JR, Sneek, The Netherlands

[∥]Department of Chemical and Environmental Engineering, Mason Lab, Yale University, 9 Hillhouse Avenue, New Haven, Connecticut 06520-8286, United States

ABSTRACT: Renewable energy can be captured from the mixing of salt and fresh water in reverse electrodialysis. This paper investigates the energy efficiency of this process for feed waters that pass a reverse electrodialysis cell once and waters that pass multiple cells or electrode segments. So far, the maximum theoretical energy efficiency was considered to be 50% when the feed waters pass a single cell once; significantly higher efficiencies could only be obtained when the waters were recirculated or passed multiple electrodes. In this study, we show that the ion transport corresponding to the obtained energy and the electromotive force mutually influence each other, which enables capture of more than 50% (even up to 95%) of the theoretical energy, even when the feedwater streams pass a reverse electrodialysis cell only once.

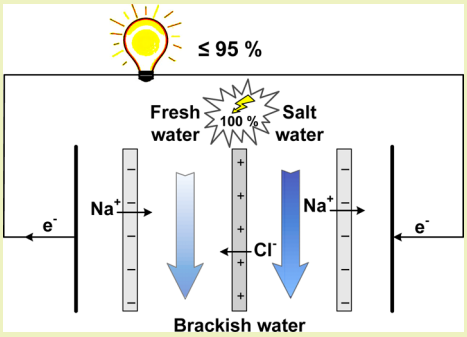

KEYWORDS: *Reverse electrodialysis, Renewable energy, Efficiency, Entropy, Salinity gradient energy, Ion exchange membranes*

INTRODUCTION

The increase in entropy upon mixing waters with different salinity gives the opportunity to capture renewable energy.[1] The potential for generating energy from salinity differences in natural waters is vast.[2,3] Theoretically, mixing seawater and river water in equal quantities would provide as much energy as the potential energy when one of these waters has a level difference of more than 150 m with respect to the other.[2,3] Several technologies are proposed to capture this energy, among others are pressure retarded osmosis (PRO),[4−6] reverse electrodialysis (RED),[7−9] and capacitive mixing (CAPMIX).[10−13]

Independent of the applied technology, a part of the theoretically available energy (i.e., exergy) is lost (even when perfect membranes are considered) if the energy is captured in a single step, i.e., when the feed flow is processed in a single stage in a continuous process. This is partly due to frictional losses (from water transport for PRO or ion transport for RED and CAPMIX) and partly due to unutilized available energy in the effluent. The latter is inevitable when a single pressure (PRO) or electrode voltage (RED and CAPMIX) is chosen to capture the energy. During operation, when the concentrations on either side of a selective membrane approach each other to a level that the required pressure or voltage cannot be generated anymore, mixing stops and part of the available energy leaves the system unutilized.

For PRO, the energy efficiency was recently evaluated,[6] concluding that theoretically up to 91% of the available energy could be obtained in a single step (constant pressure). Previous research on RED claimed that a maximum 50% of the available energy can be captured using a single electrode segment,[8,9,14−16] whereas the other 50% is dissipated due to the internal resistance of the RED cells. However, these previous calculations neglected the importance of local variations in electromotive force and electrical resistance.

In this study, we investigate the effect of local parameter variations on power generation compared to the theoretically available energy. We present a model for RED stacks to simulate the energy capture with natural salinity gradients. The energy extraction efficiencies under different flow orientations along the membrane (co-flow, cross-flow, and counter-flow) and with single or multiple electrodes pairs are compared and discussed, leading to new insights regarding the energy efficiency in RED.

THEORY

Reverse Electrodialysis (RED). A RED cell comprises membranes that are selective for cations (cation exchange membrane, CEM) or anions (anion exchange membrane, AEM),[1,7] as illustrated in Figure 1. When waters with different salinity are present on either side of a CEM or AEM, a voltage

Received: May 18, 2013
Revised: July 23, 2013
Published: August 2, 2013

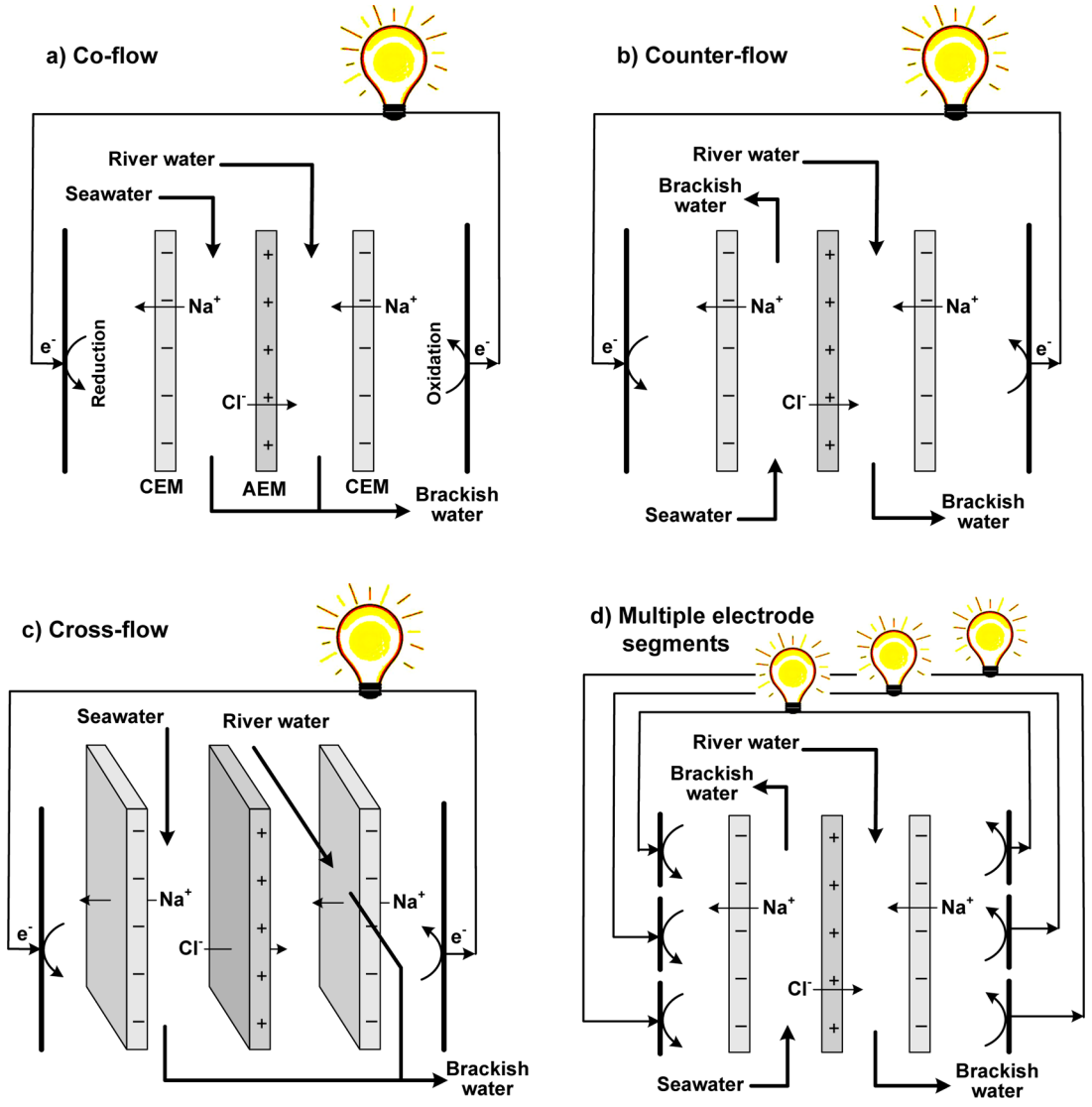

Figure 1. Principle of RED using (a) co-flow, (b) counter-flow, (c) cross-flow, and (d) counter-flow with segmented electrodes. For simplicity, each setup is presented with one RED cell only, comprised of two membranes and two compartments. Multiple cells can be stacked between the electrodes. The final membrane serves to shield the electrode rinse solution from the feedwater.

is created due to the membrane selectivity for cations or anions. This voltage, known as the Donnan potential, can be accumulated when membranes are stacked alternately with salt water and fresh water in between these membranes. Such a voltage can be used to power an electrical device when electrodes and a (reversible) redox reaction are introduced at both ends of the membrane stack.[1,7]

A RED cell can be operated in several modes. The flow of seawater and river water can be directed in the same way (co-flow, Figure 1a), in opposite direction (counter-flow, Figure 1b), or perpendicular to each other (cross-flow, Figure 1c). Some previous experimental designs for RED used co-flow[17] or counter-flow,[18] but for practical reasons most designs were based on cross-flow.[2,8,9] Additionally, the electrodes can be composed of one single part (Figure 1a–c) or multiple segments (Figure 1d). Previous research indicated that multiple electrode segments increases the overall power density.[15,18] This research will evaluate the maximum extractable energy for all cases.

Energy of Mixing. When two streams with different salinity are mixed until all available energy is released, both effluent streams attain the same salinity. In that case, the available energy is defined by the Gibbs free energy of mixing.[2,6] Including the activity coefficients that account for the non-ideality for concentrated solutions,[2,6] the theoretical obtainable energy, ΔG_{mix} (J), per mole of brackish water, n_b, is given by:

$$\frac{\Delta G_{mix}}{n_b} = -T \times (\Delta S_b - f \times \Delta S_s - (1-f) \times \Delta S_r) \quad (1)$$

$$\text{with } \Delta S = -R \times \sum_i x_i \times \ln(\gamma_i \times x_i)$$

In these equations R is the universal gas constant (8.314 J/(mol K)), T is the absolute temperature (K), f is the fraction of seawater relative to the total feed flow (-), x is the mole fraction of species i (-), and γ is the activity coefficient (-). The subscripts s, r, and b indicate seawater, river water, or brackish water, respectively. Similarly, the theoretical obtainable power $P_{\Delta G_{mix}}$ (W) is

$$\frac{P_{\Delta G_{mix}} \times V_{mol,b}}{\Phi_b} = -T \times (\Delta S_b - f \times \Delta S_s - (1-f) \times \Delta S_r) \quad (2)$$

where Φ is the volumetric flow rate (m^3/s) and $V_{mol,b}$ is the molar volume of brackish water (m^3/mol).

Following eq 2, mixing typical seawater (30 g/L NaCl) and river water (1 g/L NaCl), both at a flow rate of 1 m^3/s, would release 1.39 MW. Neglecting the mole fraction of H_2O has only a marginal effect on the released power (1.35 MW). Neglecting the activity coefficients has a slightly larger effect (1.45 MW).

Extractable Energy in RED. The actual obtained power depends on the voltage over the reverse electrodialysis cells and the electrical current through these cells. The voltage over a perfectly selective membrane (i.e., electromotive force), E (V), is given by the Nernst equation[19]

$$E = \frac{R \times T}{z \times F} \times \ln\left(\frac{\gamma_s \times c_s}{\gamma_r \times c_r}\right) \quad (3)$$

where z is the valence of the ions (-), F is the Faraday constant (96485 C/mol), and c is the salt concentration (mol/m^3). The voltage that is obtained over a cell, i.e., the electrode voltage U (V), equals the voltage over two perfectly selective membranes (one CEM and one AEM) minus the ohmic loss due to the cell resistance[7]

$$U = 2 \times E - R_{cell} \times J \quad (4)$$

where R_{cell} is the area resistance of a cell ($\Omega\ m^2$), and J is the electrical current density (A/m^2). The cell resistance is composed of the ohmic resistance of the membranes and the feedwater. The resistance of the electrodes and the additional membrane to shield the electrode compartments is negligible for large numbers of cells.[8]

The electrical current density corresponds to the local ion transport from seawater to river water. Because the feedwater compartments are elongated (i.e., the length of the flow channels is much larger than its thickness), diffusion and migration of ions can be assumed to be only perpendicular to the membrane. When further assuming a steady state and no leakage (perfect membranes), the concentration profile along the RED cell (in the direction of the flow) can be derived from two differential equations.[15] For co-flow, these equations are

$$\frac{dc_s}{dy} = -\frac{J(y) \times b}{\Phi_s \times F} \quad (5)$$

$$\frac{dc_r}{dy} = \frac{J(y) \times b}{\Phi_r \times F} \quad (6)$$

where y is the distance from the feedwater inflow (m), and b is the width of the feedwater compartments (m). J is a function of y, as it represents the local current density. Because the electrical current density is dependent on the electromotive force, which is dependent on both the salt concentration in the seawater and the river water, these differential equations are coupled.

In case of counter-flow, the same equations are valid, but the sign in either eqs 5 or 6 is reversed. For cross-flow, the derivative in eq 5 is in perpendicular direction as in eq 6, which makes eqs 5 and 6 partial differential equations in this case.

Because the concentrations are dependent on the location in the cell (y) and the electrical current through the cell, i.e., on the chosen electrode voltage (U), the electromotive force and the cell resistance are a function of y and U as well. We express that as $E(y,U)$ and $R_{cell}(y,U)$. The obtained power P (W) that is obtained at the electrodes of a RED cell is described by integration of the product of U and J and can be rewritten in terms of $E(y,U)$ and $R(y,U)$

$$P = b \times \int_0^L U \times J dy = b \times \int_0^L \frac{2E(y,U) \times U - U^2}{R_{cell}(y,U)} dy \quad (7)$$

where L is the length of the cell from inflow to outflow (m).

When the outflow concentrations of the seawater stream and the river water stream are not equal, a part of the available power is unused. This unused power is calculated using the outflow concentrations for river water and seawater and eq 2.

The energy efficiency η (-) is defined as the ratio of the actual obtained power P (W) versus the corresponding theoretical power according to the Gibbs equation ($P_{\Delta G_{mix}}$):

$$\eta = \frac{P}{P_{\Delta G_{mix}}} \times 100\% \quad (8)$$

If the electromotive force E and the internal resistance R_{cell} are independent of the electrode voltage U, the power in eq 7 would be at maximum when U equals the average of E. This implies that the electrode voltage is only 50% of the generated electromotive force, while the other 50% is lost on internal ohmic losses,[8,9,14−16] as given by

$$P_{ohmic\ loss} = b \times \int_0^L J^2 \times R_{cell} dy \quad (9)$$

If E equals U, the obtained power (eq 7) will be equal to the power lost on ohmic losses. However, because E and R_{cell} are (non-linearly) dependent on U, the relation between the power and electrode voltage U is more complex. If the electrode voltage decreases, the current density is increased, and more ions will be transported from seawater to river water. Hence, the electromotive force will decrease (i.e., $\partial E/\partial U > 0$), and the internal resistance will decrease (i.e., $\partial R_{cell}/\partial U > 0$). These feedback mechanisms imply that the maximum power can be obtained when U is different from the average of E, and the energy efficiency is not limited to 50% even for a single set of electrodes.

The ohmic losses can be reduced in any RED system by minimizing the electric currents at the expense of slower ion transport and, consequently, more available energy will leave the system unused. To capture maximum energy at low current density, RED can be applied in multiple stages. This can be done by leading the feedwater through several RED cells in series[8] or dividing the electrodes in multiple segments in series, each controlled individually[15] (Figure 1d). The current density in each stage can be kept low in such a system, as the unused energy can be captured in the next stages.

MODELING METHODOLOGY

To calculate the energy efficiency for all these cases (co-flow, cross-flow, or counter-flow, each with one single electrode pair or segmented electrode pairs), a model was designed to solve the differential eqs 5 and 6 and the corresponding maximum energy efficiency. The obtained energy was calculated by eq 7, whereas the ohmic loss was calculated by eq 9. The unused energy was calculated based on the outflow concentrations for river water and seawater and eq 2. As input parameters, a concentration of 30 g/L NaCl (0.513 M) was chosen as seawater and 1 g/L NaCl (0.017 M) was chosen as river water inflow.

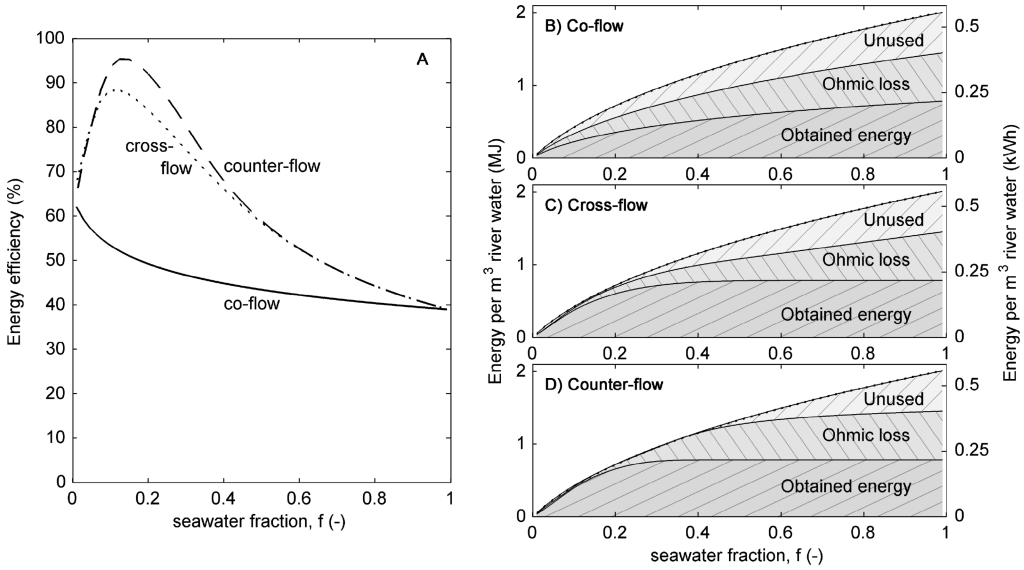

Figure 2. (A) Energy efficiency as function of the seawater fraction, $f = \Phi_{sea}/(\Phi_{sea} + \Phi_{river})$, for co-flow, cross-flow, and counter-flow. The theoretical available energy per m^3 river water is split into obtained energy, energy lost as an ohmic loss, and unused energy for (B) co-flow, (C) cross-flow, and (D) counter-flow, all as a function of the fraction of seawater. All cases use non-segmented electrodes and a fixed residence time of the river water of 30 s. A seawater fraction of $f = 0$ implies that no seawater is used, while $f = 1$ implies that an infinite amount of seawater is used.

The membranes were assumed perfect (i.e., 100% permselective and no membrane resistance), which resembles the practical case where the river water dominates the resistance R_{cell}. A cell length (distance between inflow and outflow) of 0.1 m and an intermembrane distance of 100 μm were chosen, as these values are typical for laboratory experiments.[9,20] The total electrode area at each side of the membrane pile was 10 cm × 10 cm in all cases. When using segmented electrodes, only the electrodes are segmented, in equal parts, and the total electrode area remains 10 cm × 10 cm. The electrical current is assumed only perpendicular to the electrodes, which resembles a thin membrane pile relative to the length and width. The conductivity of the feedwater in the compartments was estimated using the concentration and a molar conductivity Λ of 0.01287 S m^2/mol.[21] The activity coefficients were calculated based on the salt concentration and a modified three characteristic parameter correlation (TCPC) model.[22] Concentration changes in the boundary layer (referred to as concentration polarization) are assumed negligible. The residence time of the river water was fixed at 30 s, whereas the residence time for the seawater was varied to obtain different ratios between the feedwater flows.

The electrode voltage U was varied and optimized to obtain a maximum energy efficiency, using a Nelder–Mead simplex method.[23] In cases of segmented electrodes (Figure 1d), the voltage over each electrode segment, U, could be chosen individually. In the specific case of cross-flow with segmented electrodes, the electrodes were segmented in the direction of the river water flow, as the electromotive force is most sensitive to the concentration of the river water. Equations 1–7 were solved and optimized using Matlab (v7.7, The Mathworks). The concentration profile in the case with co-flow was solved using an ode45 solver, and the cases with counter-flow and cross-flow were solved using concentration profiles in matrices and a forward difference method. A resolution of 1000 grid points in each direction was used for the latter cases. The results were insensitive to further refinement of the step size and error tolerance.

RESULTS AND DISCUSSION

Influence of Flow Configuration. The energy efficiency for co-flow, cross-flow, and counter-flow with a non-segmented electrode are shown in Figure 2A. Figure 2B–D show the theoretical available energy per m^3 river water for all theses cases split into obtained energy, energy lost as an ohmic loss, and unused energy in the effluent. Because the river water will be limited in most practical cases, all graphs are plotted as a function of the fraction of seawater (relative to the total feed flow).

Figure 2A shows that even 95% of the theoretical available energy can be captured using only one electrode segment, for counter-flow at $f = 0.13$. This is clearly more than the previously claimed 50%[8,9,14−16] due to the interaction mechanism between electromotive force (E), electrode voltage (U), and cell resistance (R_{cell}) (eq 7). The energy efficiency for the case with counter-flow is slightly higher than for the case with cross-flow, and for some cases ($f \approx 0.15$), almost twice the available energy is captured compared to the case with co-flow.

Although highest efficiencies are obtained at low seawater fractions f, Figure 2B–D show that the obtained energy (and thus the power density) increases when f increases. For cross-flow and counter-flow, the obtained energy only slightly increases at $f > 0.3$, while for co-flow the obtained energy continues increasing for higher values of f. Figure 2B–D show that the ohmic loss as well as the unused energy is larger for co-flow at most values of f, compared to cross-flow and counter-flow. The ohmic loss and unused energy also increase in all cases when the seawater fraction increases. The additional energy that is available at increased seawater fraction cannot be used as efficiently as for low seawater fractions, as is observed in the lower efficiencies in Figure 2A with increasing f and the plateaus for cross-flow and counter-flow in Figure 2C and D. The unused energy and ohmic loss are discussed below in more detail.

Unused Energy. The unused energy is largest in the case with co-flow. When co-flow is considered, ions cannot fully exchange to a level where the salt concentrations in both outflow streams are equal because equal concentrations at either side of the membrane would correspond to a zero electromotive force close to the outflow of the cell. When a single electrode segment is used, the electromotive force needs to remain equal or larger than the electrode voltage. Therefore, part of the available energy is unused and remains in the

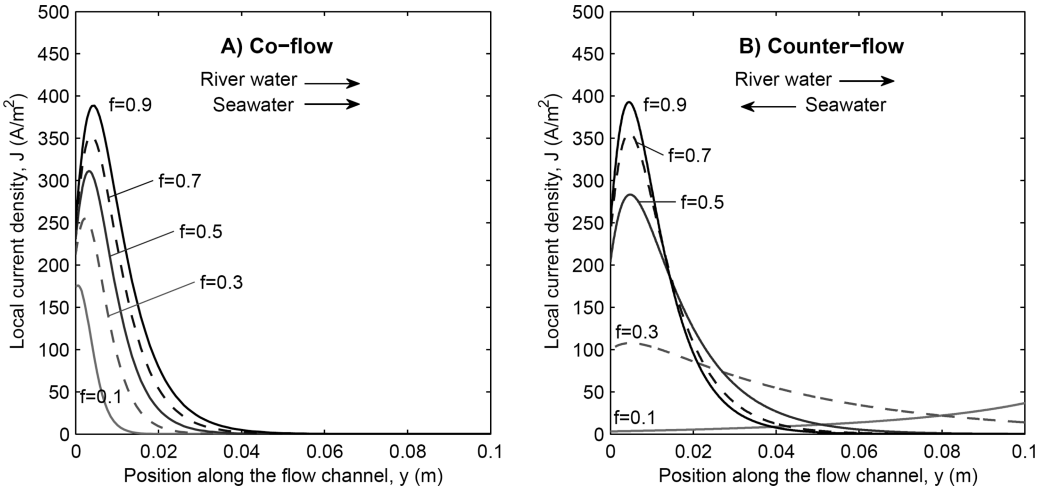

Figure 3. Local current density (J) as function of the position along the flow channels (y) for (A) co-flow and (B) counter-flow. Both panels show graphs for different seawater fractions (f). All cases use a fixed residence time of the river water of 30 s. The arrows show the flow direction for river water and seawater.

effluent in a co-flow case. Using counter-flow, the local electromotive force will remain non-zero at all positions along the flow channels, even if the outflow concentrations of both streams are equal because the outflows are positioned opposite. As a consequence, the salinity difference can be fully utilized in a counter-flow case.

The unused energy for the cross-flow case (Figure 2C), and therefore the energy efficiency (Figure 2A), is in between the values for co-flow and for counter-flow. Considering cross-flow, the ion transfer in the water near the inlet of the other stream can continue along the flow channel until the concentration of the brackish mixture is reached, as for counter-flow. However, for the feedwater that is positioned near the outflow of the other stream, the local concentration difference between the water streams is smaller, such that the electromotive force is only slightly larger than the electrode voltage. Consequently, fewer ions are transferred here, and the outflow concentration does not reach the concentration of the brackish mixture. This is reflected in the unused energy for the cross-flow case, which is higher than for the counter-flow case (Figure 2D) but lower than for the co-flow case (Figure 2B).

A small fraction of the unused energy of the cross-flow case is due to a varying concentration along the width of the river water outflow and the width of the seawater outflow. The feedwater that flows close to the inflow of the other feedwater has more ion exchange than the feedwater that flows close to the outflow of the other feedwater. As a consequence, the outflow concentrations within both feed streams vary along the width. When using a single manifold for each outflow stream, energy is lost due to irreversible mixing of the river water outflow and irreversible mixing of the seawater outflow. This effect is most pronounced close to equal flows for river water and seawater (f = 0.5), where it accounts for approximately 13% of the total available energy.

Ohmic Loss. Although the ohmic loss is, for some seawater fractions, largest for counter-flow, the co-flow has the largest ohmic loss for all seawater fractions when normalized for the obtained energy (Figure 2B). The relatively large ohmic loss for co-flow can be explained when inspecting the local current density. Figure 3 shows the local current density for co-flow and counter-flow and for several seawater fractions. The cross-flow case is shown later separately, because the water streams flow in different dimensions in the cross-flow case.

Figure 3 shows that the current density for large fractions of seawater ($f \geq 0.7$) peaks a few millimeters after the river water inflow ($y \approx 0.005$ m) both for co-flow and counter-flow, although the concentration difference between river water and seawater is even larger at y = 0. The reason is that the current density peaks slightly later because the ohmic cell resistance (R_{cell}) is also largest at y = 0 due to the low conductivity of the river water. Previous research showed that the maximum local current density (and thus the highest local power density) is obtained when the river water concentration is increased to approximately 0.030 M.[15]

For seawater fractions $\leq$ 0.5, the current density shows a distinct peak in the case of co-flow, whereas it is more equally distributed over the full channel for counter-flow. The high local current density for co-flow is a consequence of the rapidly decreasing concentration difference over the membrane as the waters flow along the channels. Because river water and seawater flow in the same direction, the (salt) enriched river water flows along the (salt) depleted seawater. This lowers the electromotive force and therefore limits the ion exchange in the case of co-flow. For counter-flow, the concentration difference over the membrane is more equally distributed because the ions that are transferred from seawater to river water are discharged in opposite direction. The distinct peak in current density for co-flow explains the higher ohmic loss, as the ohmic loss is proportional to the local current density squared (eq 9).

As the power density (i.e., power normalized for the membrane area) is proportional to the current density, Figure 3 implies that the power density also has a distinct peak near the river water inflow for most cases. A shorter residence time (i.e., faster flow rate or shorter flow channel) would significantly improve the power densities, which can result in a higher power density for co-flow compared to counter-flow.[18] The low current densities at y > 0.04 suggest that using half the residence time would significantly improve the power densities (roughly doubled), while the energy efficiency decreases less than 2%. The energy efficiency is only compromised seriously when the residence time would be more than 2.5 times smaller, which can be visualized by confining the y-axis to y < 0.04. In this range, a trade-off between high power densities and high

efficiencies is required, as was observed in previous experiments.[9,18]

Cross-flow has an even smaller ohmic loss compared to the other cases (22% of the theoretical available energy versus 32% and 37% for co-flow and counter-flow, respectively), as demonstrated in Figure 2C. To show the current density in the two-dimensional cross-flow case, the local current density is plotted against the position on the membrane in the feedwater flow channels in Figure 4 for the case of $f = 0.5$. This can be compared to the current density in the one-dimensional cases with co-flow and counter-flow for $f = 0.5$ as presented in Figure 3.

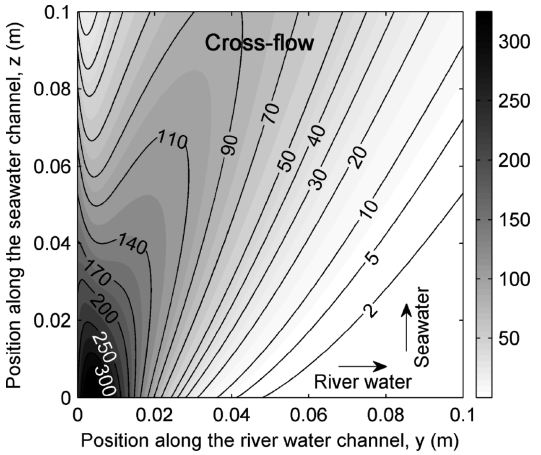

Figure 4. Local current density (J, in A/m^2) as a function of the position on the membrane in the river water and seawater compartment (y and z) for cross-flow and $f = 0.5$. The arrows show the flow direction of river water and seawater.

Figure 4 shows, in comparison to the cases in Figure 3, that the current density is more equally distributed over the membrane area for the cross-flow case, which is most pronounced compared to the case with co-flow. In other words, the peak in current density in the case with cross-flow is less distinct, and the area with a low current density is limited. This is indicated in Figure 4, for example, by a current density of approximately 15 A/m^2 near the outflow of river water and seawater, whereas the current densities near the river water outflow for the cases with co-flow and counter-flow are lower than 1 A/m^2. The reason is the larger variation (two-dimensional) in concentrations in case of cross-flow. Ion exchange can still occur even close to the outflows of both streams because the feed waters did not have major ion exchange during their past route along the membranes. Therefore, the high exchange in the area close to the outflows of both streams causes a more equal distribution of current density over the membrane area. Hence, the cross-flow case has the lowest ohmic loss at $f = 0.5$.

Considering the previous discussion, both ohmic loss and unused energy are dependent on the flow direction of the river water and seawater. Those losses are in general higher for co-flow compared to cross-flow and counter-flow due to a stronger decrease in electromotive force and therefore a more locally intensified current density in the case of co-flow.

Effect of Seawater Fraction. The same reasons for the lower energy efficiency in co-flow are applicable to the other cases when the seawater volumetric fraction (f) is increased. The energy efficiency in general decreases for increasing f (Figure 2A), which can be observed from the plateau value reached for the obtained energy for cross-flow (Figure 2C) and counter-flow (Figure 2D) at $f > 0.5$. At higher seawater fractions, the river water salinity increases faster along its path from inflow to outflow. Because the electromotive force depends on the salinity ratio (eq 3), the electromotive force is sensitive to local changes in river water concentration along the feedwater channel. The corresponding low electromotive force decreases the ion transport rate, and more energy will leave the system unused. Moreover, an excess in seawater creates a sharper peak in local current density close to the river

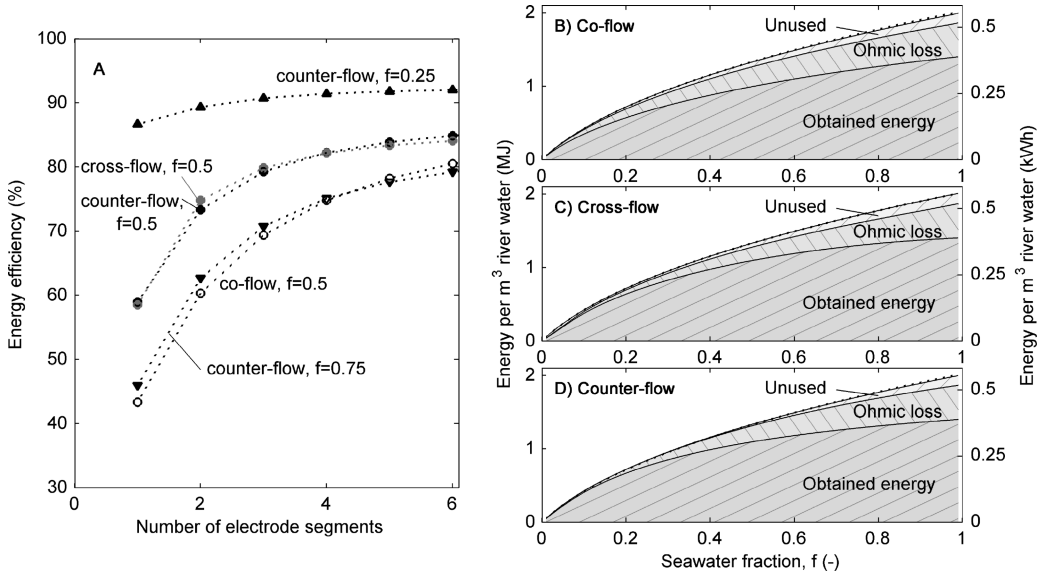

Figure 5. Energy efficiency (A) as a function of the number of electrode segments for co-flow and cross-flow with equal seawater and river water flow ($f = 0.5$) and for counter-flow where the seawater fraction varies ($f = 0.25$, 0.5, and 0.75). The theoretical available energy per m^3 river water is split into obtained energy, energy lost as an ohmic loss, and unused energy for (B) co-flow, (C) cross-flow and (D) counter-flow, all as function of the fraction of seawater and using four electrode segments. The residence time of river water was fixed to 30 s in all cases.

water inlet (Figure 3) and hence increases the ohmic loss. Therefore, the excess of seawater is not used efficiently.

At extreme cases, for fractions of seawater nearly 0 or nearly 1, one of the feed flows fully limits the power production and ion transport is limited to a small area close to that inflow only. This situation disables the benefit of a more equal distribution of ion transfer for cross-flow and counter-flow. In these cases, the energy efficiency for situations with co-flow, cross-flow, and counter-flow approach each other and the energy efficiency coincides at $f = 0$ and $f = 1$ for all cases presented in Figure 2A.

Although the highest efficiencies can be obtained for low seawater fractions, 1:1 mixing ratios or even an excess in seawater supply may be still favorable in practical situations where the river water supply is limited. The obtained energy per m^3 river water is largest for high seawater fractions. Moreover, the power density will increase even further for higher f because the same electrical current can be obtained with a smaller membrane area, as demonstrated in Figure 3, which will reduce the membrane costs.[24] The exact optimum of the seawater fraction is dependent on among others the residence time, feedwater availability, membrane pricing, and feedwater pretreatment. Therefore, the energy efficiency and obtained energy when using multiple electrode segments has been calculated for several seawater fractions.

Effect of Segmented Electrodes. To improve the obtained energy and the energy efficiency, segmented electrodes can be used. The energy efficiency is shown in Figure 5A as a function of the number of electrode segments. The obtained energy, ohmic loss, and unused energy per m^3 river water as a function of the seawater fraction when the electrodes are divided into four segments are presented in Figure 5B–D.

As expected, higher energy efficiencies can be achieved in all cases when multiple electrode segments (or multiple stacks in series) are used (Figure 5A). With multiple electrode segments, the system is divided in multiple steps, which is a basic condition for approaching a reversible process. Figure 5A shows that the case with co-flow and the case with counter-flow for $f = 0.75$ benefit most pronounced when using multiple electrode segments. In these cases, the effluent from the first electrode segment still contains a large fraction of unused energy (Figure 2) because the electromotive force (E) quickly approaches the electrode voltage (U) in these cases, which limits the ion transport. With more electrode segments, the unused available energy after the first electrode segment(s) can be used for energy generation in the next segments. Each subsequent electrode segment can operate at a lower voltage, which enables to capture the available energy from the effluent of previous electrode segments. This is demonstrated in Figure 5B–D, which shows that the unused energy is reduced to only a few percent of the total available energy when the electrodes are divided into four segments.

Furthermore, the current density in the first segments can be lower than when using only one electrode segment, which reduces the ohmic losses. The first electrode segment, where the river water compartment is weakly conductive, operates at a high electrode voltage and low current density. At the subsequent voltages, the electrode voltage is lower while the current density is higher due to a more conductive river water compartment as a result of the increased salt concentration. This strategy roughly halves the ohmic losses for a 1:1 mixture ($f = 0.5$) when using four electrode segments (Figure 5B–D) compared to using a single set of electrodes (Figure 2B–D). The ohmic loss is still lowest for the case with cross-flow (14% of the available energy for cross-flow versus 20% for co-flow and 16% for counter-flow at $f = 0.5$) due to the more uniform distribution of the current density, similar to the case with a single set of electrodes (Figures 3 and 4).

The cross-flow case has a similar energy efficiency as the counter-flow case at $f = 0.5$ using non-segmented electrodes as observed earlier (Figure 2A). The obtained energy is slightly higher for cross-flow than for counter-flow when using two and three electrode segments and slightly lower for five or more electrode segments. The benefit of cross-flow when using two or three electrode segments stems from the fact that more unused energy remains when using one electrode segment for cross-flow than for counter-flow (Figure 2C,D). This energy can still be captured when using several electrode segments. The advantage for counter-flow for five or more electrode segments is explained from the arbitrary choice of segmenting the electrodes in the direction of the river water flow only. For a large number of electrode segments, cross-flow would benefit extra if the electrodes would be segmented in the direction of the seawater too.

At an infinite number of electrode segments and an infinite long residence time, the current density can be infinitely small and the ohmic loss can be neglected (i.e., reversible process). In that case, the obtained work can be derived from the integral of the electromotive force to the transported charge, up to the point in which the effluent concentrations are equal. This yields an energy efficiency of 100%, which can be confirmed by this model, independent of the flow direction or the ratio between seawater and river water.

Even though the energy efficiency as calculated in this paper assumes ideal conditions, these results are still representative of actual (non-ideal) conditions. For example, when using a non-zero membrane resistance, the same energy efficiencies can be reached, although the residence time should be increased for this case. The extra resistance decelerates the process (i.e., lower power density) but does not cause irreversible losses. The same applies to the choice of the intermembrane distance; a larger intermembrane distance decelerates the process because of increased resistance but does not create irreversible losses. Only the transport of co-ions and water through the membranes (i.e., permselectivity <100%), which is neglected for ideal membranes as in this study, causes irreversible losses in the available energy from mixing seawater and river water. Such a loss is most pronounced for very low flow rates (e.g., an order of magnitude smaller as in this study).[20] Nevertheless, experimental results using equal flows for seawater and river water ($f = 0.5$) and a design comparable with cross-flow indicate that efficiencies as high as in this idealized study are realistic. Efficiencies of $53 \pm 5\%$[9] for non-segmented electrodes and up to 80% when the feedwater passes the electrodes multiple cycles[2] are achieved experimentally, which indicates that this irreversible loss in available energy can be limited in practice.

CONCLUSIONS

The energy efficiency of mixing seawater and river water in RED can be derived from an analytical model. Assuming ideal membranes, the energy efficiency is dependent on the ratio between the seawater and river water flow and the number of electrode segments. Energy efficiencies of 95% can be obtained when using seawater and river water flowing in opposite directions (counter-flow), even for a single electrode segment, whereas only 50% was predicted in previous studies. When

seawater and river water flow in the same direction (co-flow), lower efficiencies are obtained due to ohmic losses and more unused energy. Nevertheless, also in this case, energy efficiencies much higher than 50% can be obtained. The efficiency in the more practical case of cross-flow, where the feed waters flow in a direction of 90° with respect to each other, is up to 88%, which is only slightly lower than the value obtained for counter-flow. This is based on using an excess amount of river water compared to the seawater volume. Equal flows of seawater and river water result in lower theoretical efficiencies (45−58%), but the obtained power strongly increases in these cases when multiple electrode segments are used. This implies that high efficiencies can be obtained in energy generation from RED.

AUTHOR INFORMATION

Corresponding Author

*E-mail: d.c.nijmeijer@utwente.nl. Tel.: +31 53 489 4185.

Notes

The authors declare no competing financial interest.

ACKNOWLEDGMENTS

This research is performed at Wetsus, Technological Top Institute for Water technology (www.wetsus.nl). Wetsus is funded by the Dutch Ministry of Economic Affairs, European Union Regional Development Fund, Province of Fryslân, City of Leeuwarden, and EZ/Kompas program of the "Samenwerkingsverband Noord-Nederland". The authors are thankful for the support of the participants of the research theme "Blue Energy".

REFERENCES

(1) Pattle, R. E. Production of electric power by mixing fresh and salt water in the hydroelectric pile. *Nature* **1954**, *174* (4431), 660−660.

(2) Post, J. W.; Hamelers, H. V. M; Buisman, C. J. N. Energy recovery from controlled mixing salt and fresh water with a reverse electrodialysis system. *Environ. Sci. Technol.* **2008**, *42* (15), 5785−5790.

(3) Logan, B. E.; Elimelech, M. Membrane-based processes for sustainable power generation using water. *Nature* **2012**, *488* (7411), 313−319.

(4) Achilli, A.; Cath, T. Y.; Childress, A. E. Power generation with pressure retarded osmosis: An experimental and theoretical investigation. *J. Membr. Sci.* **2009**, *343* (1−2), 42−52.

(5) Yip, N. Y.; Tiraferri, A.; Phillip, W. A.; Schiffman, J. D.; Hoover, L. A.; Kim, Y. C.; Elimelech, M. Thin-film composite pressure retarded osmosis membranes for sustainable power generation from salinity gradients. *Environ. Sci. Technol.* **2011**, *45* (10), 4360−4369.

(6) Yip, N. Y.; Elimelech, M. Thermodynamic and energy efficiency analysis of power generation from natural salinity gradients by pressure retarded osmosis. *Environ. Sci. Technol.* **2012**, *46* (9), 5230−5239.

(7) Lacey, R. E. Energy by reverse electrodialysis. *Ocean Eng.* **1980**, *7* (1), 1−47.

(8) Veerman, J.; Saakes, M.; Metz, S. J.; Harmsen, G. J. Reverse electrodialysis: Performance of a stack with 50 cells on the mixing of sea and river water. *J. Membr. Sci.* **2009**, *327* (1−2), 136−144.

(9) Vermaas, D. A.; Saakes, M.; Nijmeijer, K. Double power densities from salinity gradients at reduced intermembrane distance. *Environ. Sci. Technol.* **2011**, *45* (16), 7089−7095.

(10) Brogioli, D. Extracting renewable energy from a salinity difference using a capacitor. *Phys. Rev. Lett.* **2009**, *058501*, 1−4.

(11) Sales, B. B.; Saakes, M.; Post, J. W.; Buisman, C. J. N.; Biesheuvel, P. M.; Hamelers, H. V. M Direct power production from a water salinity difference in a membrane-modified supercapacitor flow cell. *Environ. Sci. Technol.* **2010**, *44* (14), 5661−5665.

(12) Boon, N.; van Roij, R. "Blue energy" from ion adsorption and electrode charging in sea and river water. *Mol. Phys.* **2011**, *109* (7−10), 1229−1241.

(13) Vermaas, D. A.; Bajracharya, S.; Sales, B. B.; Saakes, M.; Hamelers, B.; Nijmeijer, K. Clean energy generation using capacitive electrodes in reverse electrodialysis. *Energy Environ. Sci.* **2013**, *6* (2), 643−651.

(14) Veerman, J.; Post, J. W.; Saakes, M.; Metz, S. J.; Harmsen, G. J. Reducing power losses caused by ionic shortcut currents in reverse electrodialysis stacks by a validated model. *J. Membr. Sci.* **2008**, *310* (1−2), 418−430.

(15) Veerman, J.; Saakes, M.; Metz, S. J.; Harmsen, G. J. Reverse electrodialysis:A validated process model for design and optimization. *Chem. Eng. J.* **2011**, *166* (1), 256−268.

(16) Kim, D.-K.; Duan, C.; Chen, Y.-F.; Majumdar, A., Power generation from concentration gradient by reverse electrodialysis in ion-selective nanochannels. *Microfluid. Nanofluid.* **2010**, *9*, (6).

(17) Vermaas, D. A.; Saakes, M.; Nijmeijer, K. Power generation using profiled membranes in reverse electrodialysis. *J. Membr. Sci.* **2011**, *385−386* (0), 234−242.

(18) Veerman, J.; Saakes, M.; Metz, S. J.; Harmsen, G. J. Electrical power from sea and river water by reverse electrodialysis: A first step from the laboratory to a real power plant. *Environ. Sci. Technol.* **2010**, *44* (23), 9207−9212.

(19) Długołęcki, P. E.; Nijmeijer, K.; Metz, S. J.; Wessling, M. Current status of ion exchange membranes for power generation from salinity gradients. *J. Membr. Sci.* **2008**, *319* (1−2), 214−222.

(20) Veerman, J.; Jong, R. M. D.; Saakes, M.; Metz, S. J.; Harmsen, G. J. Reverse electrodialysis: Comparison of six commercial membrane pairs on the thermodynamic efficiency and power density. *J. Membr. Sci.* **2009**, *343* (1−2), 7−15.

(21) Moore, W. J. *Physical Chemistry*, 5 ed.; Prentice-Hall: Upper Saddle River, NJ, 1999; p 977.

(22) Ge, X.; Wang, X.; Zhang, M.; Seetharaman, S. Correlation and prediction of activity and osmotic coefficients of aqueous electrolytes at 298.15 K by the modified TCPC model. *J. Chem. Eng. Data* **2007**, *52* (2), 538−547.

(23) Lagarias, J., C.; Reeds, J., A.; Wright, M., H.; Wright, P., E. Convergence properties of the Nelder−Mead simplex method in low dimensions. *SIAM J. Optim.* **1998**, *9* (1), 112−147.

(24) Strathmann, H. Electrodialysis, a mature technology with a multitude of new applications. *Desalination* **2010**, *264* (3), 268−288.